doi:10.1017/S0016756813000605

RAPID COMMUNICATION

The first ^{40}Ar–^{39}Ar date from Oxfordian ammonite-calibrated volcanic layers (bentonites) as a tie-point for the Late Jurassic

P. PELLENARD*†, S. NOMADE‡, L. MARTIRE§, F. DE OLIVEIRA RAMALHO¶, F. MONNA|| & H. GUILLOU‡

*Biogéosciences, CNRS-UMR 6282, Université de Bourgogne, F-21000 Dijon, France
‡LSCE-IPSL, CNRS-UMR 8212, CEA Orme, F-91191 Gif-sur-Yvette, France
§Dipartimento di Scienze della Terra, University of Torino, via Valperga Caluso 35 10125 Torino, Italy
¶Statoil ASA, Grenseveien 21, 4313 Forus, Norway
||ARTeHIS, CNRS-UMR 6298, Université de Bourgogne, F-21000 Dijon, France

(*Received* 26 December 2012; *accepted* 1 July 2013)

Abstract

Eight volcanic ash layers, linked to large explosive events caused by subduction-related volcanism from the Vardar Ocean back-arc, interbedded with marine limestones and cherts, have been identified in the Rosso Ammonitico Veronese Formation (northeastern Italy). The thickest ash layer, attributed to the *Gregoryceras transversarium* ammonite Biozone (Oxfordian Stage), yields a precise and reliable ^{40}Ar–^{39}Ar date of 156.1 ± 0.89 Ma, which is in better agreement with GTS2004 boundaries than with the current GTS2012. This first biostratigraphically well-constrained Oxfordian date is proposed as a new radiometric tie-point to improve the Geologic Time Scale for the Late Jurassic, where ammonite-calibrated radiometric dates are particularly scarce.

Keywords: geochronology, palaeovolcanism, bentonite, Oxfordian, Jurassic Time Scale.

1. Introduction

There are no well-constrained radiometric dates, closely tied to ammonite biostratigraphy, currently available for the whole of the Upper Jurassic (Gradstein *et al*. 2012). Some Upper Jurassic Ar–Ar dates are integrated as secondary guides into the GTS2012: (1) a suite of dates from the almost totally non-marine Morrison Formation in the USA (Gradstein, Ogg & Smith, 2004; Ogg, Ogg & Gradstein, 2008); (2) dates from Oxfordian tuffs intercalated with terrestrial sediments in China (Chang *et al*. 2009); and (3) dates from ocean-floor basalt veins in the Pacific (Gradstein *et al*. 2012). A single Re–Os date is available from ammonite-bearing marine sedimentary successions in the Lower Kimmeridgian (Selby, 2007). As a consequence, the Late Jurassic Time Scale derives mainly from the Pacific seafloor-spreading numerical model of the M-sequence magnetic polarity pattern and from limited recent cyclostratigraphic studies (Ogg & Smith, 2004; Ogg *et al*. 2010; Gradstein *et al*. 2012). Magnetostratigraphy can be calibrated with ammonite assemblage biochronology, which is mainly defined in northwestern European domains (Cariou & Hantzpergue, 1997; Morton, 2006). However, provincialism in Boreal, sub-Boreal, sub-Mediterranean and Tethyan domains prevents unequivocal zonation correlation, especially for certain intervals, and hence introduces a temporal bias in the magnetostratigraphic model. Despite recent progress in reducing this bias (Ogg *et al*. 2010; Przybylski *et al*. 2010; Gradstein *et al*. 2012), the scarcity of interbedded volcanic units in ammonite-bearing marine successions hinders the accurate numerical calibration of the Late Jurassic Time Scale, even with the progress made in the GTS2012, including improved numerical ages for stage boundaries, obtained by selecting only single-zircon U–Pb ages, recalculating ^{40}Ar–^{39}Ar dates and more precise magnetostratigraphy and cyclostratigraphy.

Therefore, to obtain radiometrically calibrated tie-points for the Late Jurassic, biostratigraphically constrained volcanic ash layers in Tethyan basins have been studied (Pellenard *et al*. 2003; Pellenard & Deconinck, 2006). Here, we focus on eight volcanic ash layers, weathered into bentonites, sampled in pelagic cherty limestones from the Altopiano di Asiago (Trento Plateau domain, northeastern Italy; Bernoulli & Peters, 1970; Martire, 1996). We present a new ^{40}Ar–^{39}Ar radiometric date from one of these bentonites, providing the first radiometric tie-point from biostratigraphically well-constrained sedimentary strata for the Middle Oxfordian and discuss these volcanic events and their potential sources.

2. Material and method

Six bentonite layers were identified by their field characteristics, mineralogy and geochemical features at the Serrada section and a further five, 28 km away, at the Echar and Kaberlaba sections, in the Altopiano di Asiago (Trentino Alto Adige and Veneto regions, Italy; Fig. 1a). Weathering of volcanic ashes into clays produced bentonite deposits during the early stages of diagenesis at the sediment/seawater interface. In the Rosso Ammonitico Veronese (RAV), bentonites appear as continuous, centimetre-thick red or white plastic clay-rich horizons, interbedded with limestones and cherts (Figs 1b, 3a). The RAV is an Upper Bajocian to Tithonian pelagic limestone succession, which can be divided into three units (Figs 1b, 2a; Sarti, 1985; Martire, 1992; Martire *et al*. 2006). The lower unit (Rosso Ammonitico Inferiore: RAI) and the upper unit (Rosso Ammonitico Superiore: RAS) are

†Author for correspondence: Pierre.Pellenard@u-bourgogne.fr

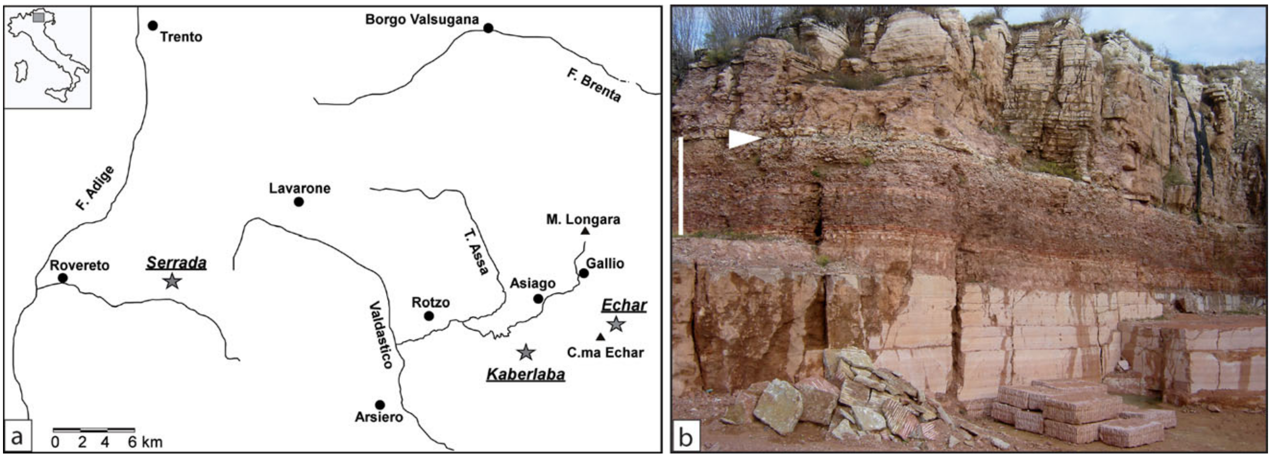

Figure 1. (Colour online) (a) Locality map of the sections sampled in the Altopiano di Asiago region: Kaberlaba (45° 50′ 27.38″ N, 11° 29′ 47.56″ E), Echar (45° 51′ 21.24″ N, 11° 34′ 44.47″ E) and Serrada (45° 53′ 16.10″ N, 11° 09′ 12.40″ E); (b) view of the three members of the Rosso Ammonitico Veronese (RAV) in the Kaberlaba quarry. Scale bar corresponds to 5.2 m, the thickness of the middle unit (RAM). The RAM unit contains typical chert layers and several bentonite layers. The position of the thickest bentonite AB4 is indicated (white arrow).

composed of massive nodular limestones, while the Rosso Ammonitico Middle unit (RAM), containing all the bentonite layers, consists of thin, evenly bedded, non-nodular, chert-rich limestones. The RAM unit reaches a maximum thickness of 10 m, although it occasionally thins out and disappears (Martire, 1996; Fig. 2a).

Mineralogical (X-ray diffraction, Biogéosciences, Dijon, France) and elemental analyses (inductively coupled plasma-optical emission spectrometry (ICP-OES) and inductively coupled plasma-mass spectrometry (ICP-MS), CRPG Nancy, France) were performed on all powdered samples to confirm their volcanic nature (online Supplementary Material Table S1 available at http://journals.cambridge.org/geo). Principal Component Analysis (PCA) was used to evaluate the number of volcanic events. Prior to the correlation matrix-based PCA, trace element concentrations were re-expressed assuming an initial volcanic concentration of 15 % Al_2O_3 (Spears *et al*. 1999; Pellenard *et al*. 2003). This procedure reduces variability in lithophile element concentration, which could be owing to post-depositional diagenetic processes, such as dilution by authigenic phases, or concentration by dissolution of less stable minerals.

The ^{40}Ar–^{39}Ar dating (OSIRIS reactor CEA Saclay, France) was performed by step-heating about 30 small (< 100 μm) transparent sanidines, carefully hand-picked under a binocular microscope after several treatments from the Kaberlaba section AB4 bentonite (original sample weight 2 kg, see online Supplementary Material available at http://journals.cambridge.org/geo for details). Each Ar isotope measurement consists of 20 cycles by peak switching between the different Ar isotopes. The J value was determined using three single ACs (Alder Creek sanidine) grains taken from the same hole as the sample. Recently, Renne *et al*. (2010, 2011) published an optimization model for estimating the partial decay constants of ^{40}K and ^{40}Ar*/^{40}K ratio of FCs (Fish Canyon sanidine). This calibration reduces systematic uncertainties in the ^{40}Ar–^{39}Ar system from *c*. 2.5 % (Steiger & Jäger, 1977) to 0.27 %. The optimization model yields an age for ACs of 1.2056 Ma, equivalent to FCs of 28.294 Ma, that overlaps at the 2σ confidence level the astronomically tuned ACs and FCs ages reported by Kuiper *et al*. (2008). The optimization model of Renne *et al*. (2010, 2011) used pairs of ^{238}U–^{206}Pb and ^{40}Ar–^{39}Ar data as inputs. Therefore, ^{40}Ar–^{39}Ar ages calibrated with this optimization model could be directly compared to U–Pb. The corresponding J value (0.0006846 ± 0.00000137, 2σ) was calculated using the Renne *et al*. (2011) calibration of ACs. The J uncertainty corresponds to the standard deviation of the weighted mean of three ACs single grains (see Nomade *et al*. 2010, 2011 and online Supplementary Material available at http://journals.cambridge.org/geo for detailed methodology).

3. Biostratigraphy and correlation of ash layers

At Kaberlaba, calcareous nannofossil assemblages indicate a Late Callovian age for the base of the RAM unit, while the ammonite assemblage composed of *Gregoryceras fouquei*, *Passendorferia* (*Enayites*) *birmensdorfensis*, *Passendorferia* cf. *ziegleri*, *Perisphinctes* (*Otosphinctes*) *nectobrigensis*, *Perisphinctes* (*Dichotomosphinctes*) aff. *elisabethae*, *Sequeirosia* (*Gemmellarites*) aff. *trichoplocus* and *Subdiscosphinctes richei*, which is characteristic of the *Gregoryceras transversarium* Biozone, indicates a Middle Oxfordian age for the top of the RAM unit (Clari, Martire & Pavia, 1990; Martire, 1992, 1996; Martire *et al*. 2006; see Fig. S1 in online Supplementary Material available at http://journals.cambridge.org/geo for photographs of typical ammonites of the *G. transversarium* Biozone). All these ammonite taxa come from the bed between bentonites AB3 and AB4 at Kaberlaba, where preservation is better than in the rest of the section. They are all exclusive to the *G. transversarium* Biozone, except for *G. fouquei*, which spans both the *G. transversarium* Biozone and the *Perisphinctes* (*Dichotomoceras*) *bifurcatus* Biozone. The overlying RAS unit contains ammonites such as *Orthosphinctes* (*Ardescia*) gr. *inconditus*, *Crussoliceras aceroides* and *Idoceras* (*Lessiniceras*) sp., which are characteristic of the *Taramelliceras strombecki* and *Presimoceras herbichi* biozones of the Lower Kimmeridgian (Sarti, 1993; Clari, Martire & Pavia, 1990; Martire, 1992, 1996). Therefore, at Kaberlaba, there is a major hiatus (four ammonite biozones) between the upper part of the Middle Oxfordian and the lowermost part of the Lower Kimmeridgian (Fig. 2a). However, the RAM unit of the Echar section provides a good biostratigraphic framework for bentonites AB4 and AB5, as here the overlying sediments are well dated, with no hiatus. The RAM unit at Echar contains the same five bentonites and is overlain by three stromatolitic beds, the first of which belongs to the *G. transversarium* Biozone, with the same taxa

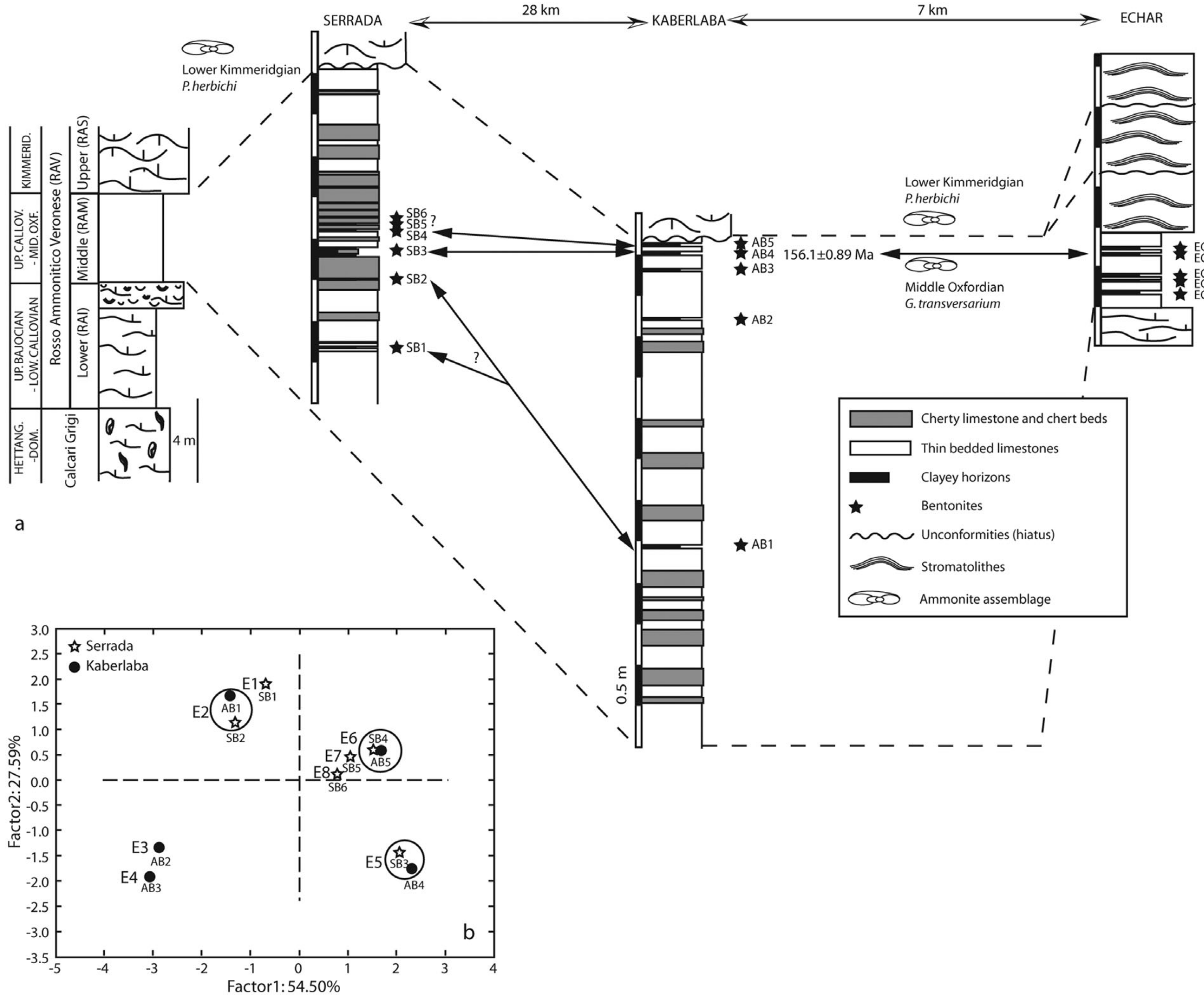

Figure 2. (a) Detailed logs of the three sections measured, showing correlations between bentonite layers and the ^{40}Ar–^{39}Ar dated AB4 bentonite (Kaberlaba), attributed to the *G. transversarium* Biozone. (b) PCA based on Al_2O_3-normalized Hf, Ga, Th, Ta, La, Zr and Ti concentrations. Circles correspond to proposed correlations between bentonite layers. E1 to E8 number the volcanic events.

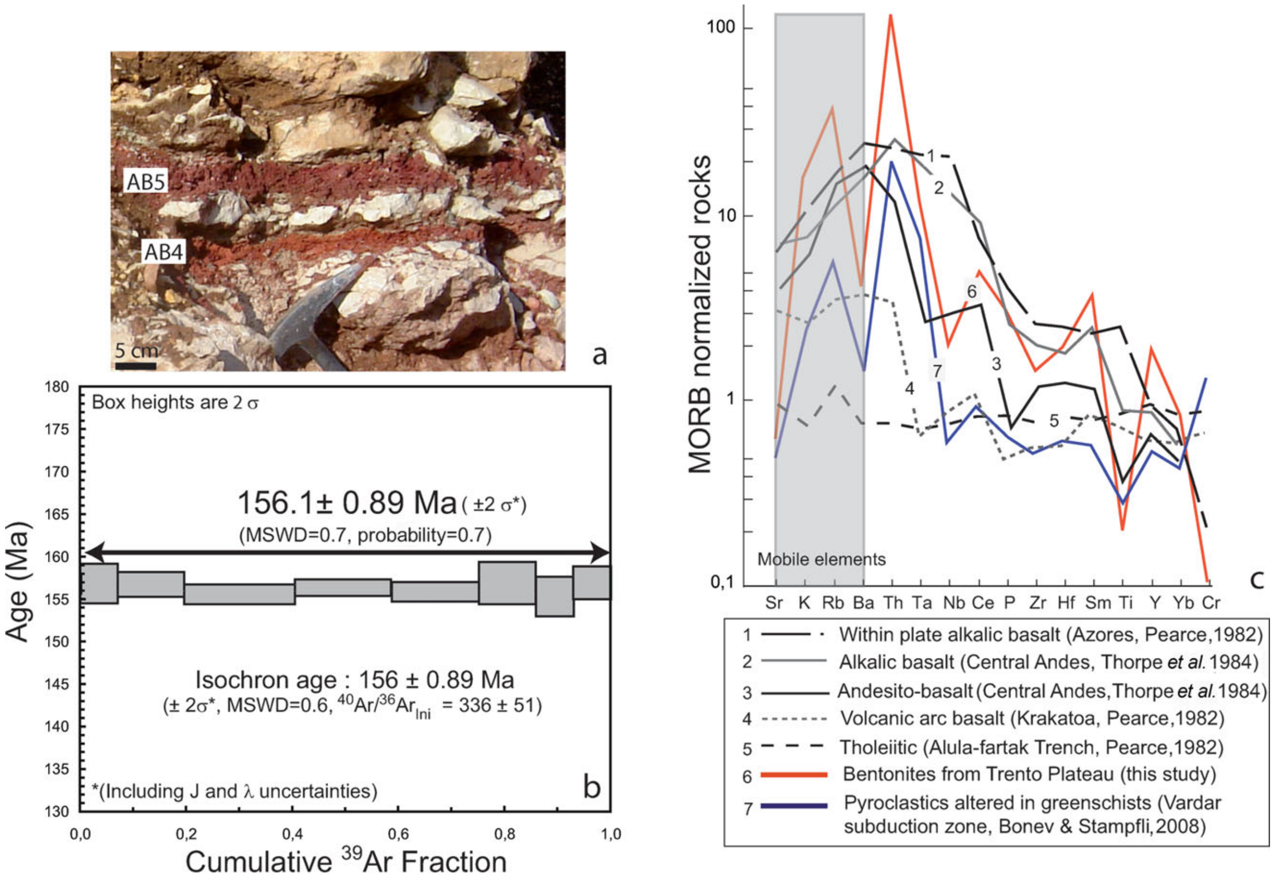

Figure 3. (Colour online) (a) Photograph of AB4 and AB5 bentonites intercalated between nodular limestones of the RAM unit (Middle Oxfordian) and overlain by the unconformity between the RAM and RAS units. (b) Apparent age spectra for AB4, showing a well-defined plateau age of 156.1 ± 0.89 Ma (2σ external). (c) MORB-normalized multi-element diagram for bentonite layers, pyroclastic deposits from the Vardar domain and comparative patterns for standard rocks from various geodynamic contexts.

as Kaberlaba. The second stromatolitic bed is dated to the Lower Kimmeridgian (*Sowerbyceras silenum* Biozone), on the basis of the following assemblage: *Taramelliceras* cf. *rigidum*, *Idoceras* (*Lessiniceras*) cf. *raschii*, *Lithacosphinctes* cf. *stromeri*, *Mesosimoceras evolutum* and *Euaspidoceras* (*Epaspidoceras*) sp. The third stromatolitic bed belongs to the *P. herbichi* Biozone (Lower Kimmeridgian, Fig. 2a). In the Serrada section, the RAM unit extends from the Upper Callovian to the Middle Oxfordian (*G. transversarium* Biozone). As all bentonites sampled were from the RAM unit, they therefore date from the Upper Callovian to the Middle Oxfordian. As ammonites diagnostic of the *G. transversarium* Biozone were found just below AB4 at Kaberlaba and just above AB5 at Echar, the two uppermost bentonite beds in these sections (AB4 and AB5), easily recognizable because of their thickness and vivid red colour (Fig. 3a), are attributed to the *G. transversarium* Biozone (Fig. 2a).

The bentonites studied, which correspond to pure smectite horizons containing occasional volcanic crystals (e.g. sanidine, quartz, biotite), are marked by positive anomalies in Th, Ta, Hf and Ga, characteristic of bentonite deposits (Spears *et al*. 1999; Pellenard *et al*. 2003; Table S1 in online Supplementary Material available at http://journals.cambridge.org/geo). PCA was used to examine possible similarities between ash layers in the Serrada and Kaberlaba sections, 28 km apart, in order to correlate the bentonites and to evaluate the number of volcanic events and their preservation in the Trento Plateau domain. The most typically immobile, volcanogenic elements were selected for this analysis: Hf, Ga, Th, Ta, La, Zr and Ti (Fig. 2b). In the F2 *v*. F1 diagram (Fig. 2b), representing more than 80 % of the total variance, four groups consistent with the stratigraphy can be clearly identified: (i) AB2, AB3, (ii) SB1, SB2, AB1, (iii) SB3, AB4, and (iv) SB4, SB5, SB6, AB5. The first Kaberlaba level, AB1, corresponds either to the first Serrada level SB1 or possibly to SB2. Samples AB2 and AB3 (Kaberlaba) have no equivalents in the Serrada section, indicating that these events were not systematically preserved. Sample AB4, a thick red bentonite from Kaberlaba, is geochemically similar to SB3, the thickest bentonite from Serrada. Sample AB5 from Kaberlaba probably corresponds to SB4, perhaps to SB5 or SB6. At least eight individual volcanic events are therefore identified using PCA (Fig. 2b), with correlations over a large geographic area, coherent with the biostratigraphic framework.

4. ^{40}Ar–^{39}Ar results

We used the laser-fusion step-heating ^{40}Ar–^{39}Ar method to date level AB4, which contains the highest abundance of well-preserved sanidines and which is also biostratigraphically the most precisely constrained. The apparent age spectrum obtained for the AB4 sanidines is 100 % concordant (Fig 3b, details in online Supplementary Material Tables S2 and S3 available at http://journals.cambridge.org/geo): all steps yield indistinguishable ages, with a well-defined plateau age of 156.1 ± 0.89 Ma (2σ full uncertainty propagation). As the inverse isochron displays low scatter because of its highly radiogenic content, it was not used, given the imprecise initial atmospheric ^{40}Ar/^{36}Ar ratio obtained. The plateau age we obtain can be directly compared to U–Pb ages available for the Jurassic Time Scale (GTS2004, GTS2012 and Pálfy, 2008).

Table 1. Calculated ages and corresponding uncertainties using various K total decay constants

K total decay constant	Steiger & Jäger (1977)	Steiger & Jäger (1977)	Renne *et al.* (2011)
Standard used	ACs (1.194 Ma) (1)	ACs (1.201 Ma) (2)	ACs (1.206 Ma) (3)
Equivalent FCs age	28.02 Ma	28.20 Ma	28.29 Ma
Age (Ma)	154.6	155.6	156.1
2σ (Ma)*	4.0	4.0	0.89

*The uncertainty reported is the full propagated uncertainty. (1) – Nomade *et al.* (2003); (2) – Kuiper *et al.* (2008); (3) – Renne *et al.* (2011). ACs – Alder Creek sanidine; FCs – Fish Creek sanidine.

We, however, present alternative calculations (Table 1) using several standards (Nomade *et al.* 2005; Kuiper *et al.* 2008) and total ^{40}K decay constants (Steiger & Jäger, 1977; Renne *et al.* 2011) since the Mesozoic GSSP time scale (GTS2004 and GTS2012) was based on many ^{40}Ar–^{39}Ar ages, using different ^{40}K constant and various standards. The full uncertainty propagation of the Steiger & Jäger (1977) ^{40}K total decay constant (*c.* 2.5 % at 2σ) results in an AB4 error of about 4.0 Ma, while the Min *et al.* (2000) ^{40}K decay constant, proposed by Kuiper *et al.* (2008), could not be retained because of its high degree of uncertainty of 3.9 % at 2σ, compared to the 0.57 % from Renne *et al.* (2010, 2011) that has been adopted in this study.

5. Nature and source of volcanic events

The bentonite profile in the MORB-normalized multi-element plot clearly shows that the initial ash layers result from an evolved calc-alkaline magma (Fig. 3c and online Supplementary Material Fig. S2 available at http://journals.cambridge.org/geo). The characteristic Nb depletion and the Hf–Th–Ta diagram are typical of subduction-related arc materials, while the Zr/TiO_2 *v.* Nb/Y diagram indicates mainly andesite to rhyodacite products (online Supplementary Material Fig. S2 available at http://journals.cambridge.org/geo). As no lavas or thick pyroclastic deposits have been identified in or nearby the Trento domain within the Upper Jurassic (Bernoulli & Peters, 1970; Pellenard *et al.* 2003), sources must be distant. In addition, fine-grained ashes emitted by highly explosive eruptions are known to be distributed over long distances (> 1000 km). This hypothesis is supported by (i) the correlation indicated by the PCA of several events with similar features (e.g. thickness), over a large area in the Venetian Pre-Alps, and (ii) the size (50–100 μm) of the preserved pyroclastic minerals (i.e. sanidine and quartz). Emissions of tholeiitic basalts, andesites and pyroclastites are reported for the Middle–Late Jurassic from the island-arc magmatism in the eastern Rhodope–Thrace region in Bulgaria and Greece (Bonev & Stampfli, 2008). This volcanism was associated with the southward subduction of the Meliata–Maliac Ocean under the supra-subduction back-arc Vardar Ocean/island-arc system (Bonev & Stampfli, 2008). The Vardar geodynamic context undoubtedly produced huge eruptions and subsequent widespread ashes. The age of the Vardar subduction, ranging from the Early Jurassic incipient proto-arc to the Middle–Late Jurassic arc–back-arc spreading, is coherent with the biostratigraphic age of the bentonites studied here, whose geochemical fingerprint is similar to that of the Vardar pyroclastics (Fig. 3c). This evidence supports Vardar island-arc volcanism as the probable source of the ash layers found in the Venetian Pre-Alps.

6. A new tie-point for the Late Jurassic Time Scale

There are few biostratigraphically well-constrained radiometric tie-points for the Middle–Late Jurassic. For the Middle Jurassic, the only available U–Pb ages are from (i) British Columbia bentonites, ascribed to the early Late Bathonian (Pálfy, 2008), and (ii) an ash layer (164.6 ± 0.2 Ma) in the Neuquén province (Argentina), at the Bathonian–Callovian boundary (Kamo & Riccardi, 2009). There are no biostratigraphically well-constrained radiometric ages for the Oxfordian–Tithonian interval, while only a few ^{40}Ar–^{39}Ar dates from oceanic basalts are retained in the current GTS2012: (i) 159.86 ± 3.33 (2σ) Ma and 161.17 ± 0.74 (2σ) Ma from Pacific tholeiitic basalts (site 801) assigned to the Oxfordian, based on radiolarian calibration, (ii) a revised 156.3 ± 3.4 (2σ) Ma reported for the Hawaiian basalt seafloor (site 765), correlated to the base of the Kimmeridgian (*P. baylei* ammonite zone) using the M26r magnetochron (Gradstein *et al.* 2012, appendix 2, p. 1045), and (iii) an earliest Berriasian ^{40}Ar–^{39}Ar date of 145.5 ± 0.8 (2σ) Ma from an oceanic basalt sill in the Pacific Ocean (Mahoney *et al.* 2005). Robust ^{40}Ar–^{39}Ar ages of 160.7 ± 0.4 (2σ) Ma and 158.7 ± 0.6 (2σ) Ma have recently been obtained from two tuffs in the Lanqi Formation in northeastern China, but the terrestrial fossils do not allow the attribution of a more precise stratigraphy than a Late Jurassic age (Chang *et al.* 2009). The only biostratigraphically well-constrained age, documented by Selby (2007) on an organic-rich mudrock deposit from the Isle of Skye (Scotland), yields a Re–Os age of 154.1 ± 2.2 Ma (2σ) in the Lower Kimmeridgian, just above the proposed Oxfordian/Kimmeridgian GSSP.

As a consequence, Middle–Upper Jurassic biozone duration and stage boundary ages are mainly estimated from secondary radiometric guides, indirect methods and mathematical interpolations. These approaches combine a magnetostratigraphic age model based on the cycle-scaling of the M-sequence spreading rate model correlated to the magnetostratigraphy of outcrops (Ogg *et al.* 2010; Przybylski *et al.* 2010; Gradstein *et al.* 2012) and cycle-derived durations of ammonite zones from cyclostratigraphy (Boulila *et al.* 2008, 2010; Ogg, Ogg & Gradstein, 2008; Huang, Hesselbo & Hinnov, 2010; Gradstein *et al.* 2012). Cyclostratigraphy from SE France has considerably modified ammonite biozone durations. Using a condensed section in Britain, the entire Oxfordian stage had previously been fixed at 0.6 Ma, in the GTS2004. New data from cyclostratigraphy suggest that the Oxfordian spanned 6.0 Ma, with 2 Ma attributed to the *Quenstedtoceras mariae* Zone alone (Boulila *et al.* 2008; Gradstein *et al.* 2012). The age of the Oxfordian/Kimmeridgian boundary is now set at 157.3 ± 1.0 Ma in the GTS2012, whereas it was 155.6 ± 4.0 Ma in the GTS2004 and GTS2008 (Gradstein, Ogg & Smith, 2004; Ogg, Ogg & Gradstein, 2008). In this study, the ^{40}Ar–^{39}Ar age of 156.1 ± 0.89 Ma (2σ full uncertainty propagation), attributed to the *G. transversarium* Biozone (Middle Oxfordian), is consistent with the existing Re–Os age and the ^{40}Ar–^{39}Ar ages retained as secondary guides in the GTS2012. Nevertheless, it falls outside of the current base and top limits of the *G. transversarium* Biozone proposed, respectively, at 160.09 ± 1.0 Ma (2σ) and 159.44 ± 1.0 Ma (2σ), both interpolated from Oxfordian stage boundaries (Gradstein *et al.* 2012). The age proposed here remains compatible with the Oxfordian boundaries (163.5 ± 1.1 Ma and 157.3 ± 1.0 Ma) proposed by the GTS2012 if maximum uncertainties are taken into account. However, there is a better fit with the previous Oxfordian base (161.2 ± 4.0 Ma) and top (155.6 ± 4.0 Ma) from the GTS2004 and GTS2008, where the proposed boundaries were around 2 Ma younger.

The age proposed here, well constrained within the standard Jurassic biostratigraphic zonation (Cariou & Hantzpergue, 1997), provides the first accurate and reliable numerical age currently available for the Late Jurassic Time Scale. This precise new tie-point can be used to anchor floating cyclostratigraphy and magnetostratigraphy, thus contributing to the improvement of seafloor-spreading models and, above all, will aid in the calibration of the Late Jurassic Time Scale.

Acknowledgements. This work was supported by the Centre National de la Recherche Scientifique and the Commissariat à l'Energie Atomique et aux énergies alternatives. The authors thank Carmela Chateau-Smith for English proofreading. We are grateful to J. F. Deconinck and D. Bernoulli for support and discussions about bentonites and G. Pavia and G. Meléndez for help with ammonite biostratigraphy. We particularly thank the reviewers A. L. Coe and F. Jourdan whose constructive criticisms and detailed remarks have greatly contributed to improve the manuscript.

References

BERNOULLI, D. & PETERS, T. 1970. Traces of rhyolitic-trachytic volcanism in the Upper Jurassic of the Southern Alps. *Eclogae geologica Helvetica* **63**, 609–21.

BONEV, N. & STAMPFLI, G. 2008. Petrology, geochemistry and geodynamic implications of Jurassic island arc magmatism as revealed by mafic volcanic rocks in the Mesozoic low-grade sequence, eastern Rhodope, Bulgaria. *Lithos* **100**, 210–33.

BOULILA, S., HINNOV, L., HURET, E., COLLIN, P. Y., GALBRUN, B., FORTWENGLER, D., MARCHAND, D. & THIERRY, J. 2008. Astronomical calibration of the Early Oxfordian (Vocontian and Paris basins, France): consequences of revising the Late Jurassic time scale. *Earth and Planetary Science Letters* **276**, 40–51.

BOULILA, S., DE RAFÉLIS, M., HINNOV, L., GARDIN, S., GALBRUN, B. & COLLIN, P. Y. 2010. Orbitally forced climate and sea-level changes in the Paleoceanic Tethyan domain (marl-limestone alternations, Lower Kimmeridgian, SE France). *Palaeogeography, Palaeoclimatology, Palaeoecology* **292**, 57–70.

CARIOU, E. & HANTZPERGUE, P. 1997. *Biostratigraphie du Jurassique Ouest-Européen et Méditerranéen: Zonations Parallèles et Distribution des Invertébrés et Microfossiles*. Bulletin des Centres de Recherches Exploration–Production Elf-Aquitaine, Mémoire 17, 422 pp.

CHANG, S., ZHANG, H., RENNE, P. & FANG, Y. 2009. High-precision $^{40}Ar/^{39}Ar$ age constraints on the basal Lanqi Formation and its implications for the origin of angiosperm plants. *Earth and Planetary Science Letters* **279**, 212–21.

CLARI, P. A., MARTIRE, L. & PAVIA, G. 1990. L'unità Selcifera del Rosso Ammonitico Veronese (Alpi Meridionali). In *Atti Convegno "Fossili, Evoluzione, Ambiente": Pergola II 1987* (eds G. Pallini, F. Cecca, S. Cresta & M. Santantonio), pp.151–62.

GRADSTEIN, F. M., OGG, J. G. & SMITH, A. G. 2004. *A Geologic Time Scale 2004*. Cambridge: Cambridge University Press, 589 pp.

GRADSTEIN, F. M., OGG, J. G., SCHMITZ, M. D. & OGG, G. M. 2012. *The Geologic Time Scale 2012*. Oxford: Elsevier, 1144 pp.

HUANG, C., HESSELBO, S. P. & HINNOV, L. 2010. Astrochronology of the late Jurassic Kimmeridge Clay (Dorset, England) and implications for Earth system processes. *Earth and Planetary Science Letters* **289**, 242–55.

KAMO, S. L. & RICCARDI, A. 2009. A new U-Pb zircon age for an ash layer at the Bathonian-Callovian boundary, Argentina. *GFF* **131**, 177–82.

KUIPER, K. F., DEINO, A., HILGEN, F. J., KRIJGSMAN, W., RENNE, P. R. & WIJBRANS, J. R. 2008. Synchronizing rock clocks of earth history. *Science* **320**, 500–4.

MAHONEY, J. J., DUNCAN, R. A., TEJADA, M. L. G., SAGER, W. W. & BRALOWER, T. J. 2005. Jurassic-Cretaceous boundary age and mid-ocean-ridge-type mantle source for Shatsky Rise. *Geology* **33**, 185–8.

MARTIRE, L. 1992. Sequence stratigraphy and condensed pelagic sediments. An example from the Rosso Ammonitico Veronese, northeastern Italy. *Palaeogeography, Palaeoclimatology, Palaeoecology* **94**, 169–91.

MARTIRE, L. 1996. Stratigraphy, facies and sedimentary tectonics in the Jurassic Rosso Ammonitico Veronese (Altopiano di Asiago, NE Italy). *Facies* **35**, 209–36.

MARTIRE, L., CLARI, P., LOZAR, F. & PAVIA, G. 2006. The Rosso Ammonitico Veronese (Middle-Upper Jurassic of the Trento Plateau): a proposal of lithostratigraphic ordering and formalization. *Rivista Italiana di Paleontologia e Stratigrafia* **112**, 227–50.

MIN, K. W., MUNDIL, R., RENNE, P. R. & LUDWIG, K. R. 2000. A test for systematic errors in Ar-40/Ar-39 geochronology through comparison with U/Pb analysis of a 1.1-Ga rhyolite. *Geochimica and Cosmochimica Acta* **64**, 73–98.

MORTON, N. 2006. Chronostratigraphic units in the Jurassic and their boundaries: definition recognition and correlation, causal mechanism. *Progress in Natural Science* **16**, 1–11.

NOMADE, S., GAUTHIER, A., GUILLOU, H. & PASTRE, J. F. 2010. $^{40}Ar/^{39}Ar$ temporal framework for the Alleret maar lacustrine sequence (French Massif-Central): volcanological and paleoclimatic implications. *Quaternary Geochronology* **5**, 20–7.

NOMADE, S., MUTTONI, G., GUILLOU, H., ROBIN, E. & SCARDIA, G. 2011. First $^{40}Ar/^{39}Ar$ age of the Ceprano man (central Italy). *Quaternary Geochronology* **6**, 453–7.

NOMADE, S., RENNE, P. R., VOGEL, N., DEINO, A. L., SHARP, W. D., BECKER, T. A., JAOUNI, A. R. & MUNDIL, R. 2005. Alder Creek sanidine (ACs-2): a Quaternary 40Ar/39Ar dating standard tied to the Cobb Mountain geomagnetic event. *Chemical Geology* **218**, 315–38.

OGG, J. G., COE, A. L., PRZYBYLSKI, P. A. & WRIGHT, J. K. 2010. Oxfordian magnetostratigraphy of Britain and its correlation to Tethyan regions and Pacific marine magnetic anomalies. *Earth and Planetary Science Letters* **289**, 433–48.

OGG, J. G., OGG, G. & GRADSTEIN, F. M. 2008. *The Concise Geological Time Scale*. Cambridge: Cambridge University Press, 177 pp.

OGG, J. G. & SMITH, A. G. 2004. The geomagnetic polarity time scale. In *A Geological Time Scale 2004* (eds F. M. Gradstein, J. G. Ogg & A. Smith), pp. 63–86. Cambridge: Cambridge University Press.

PÁLFY, J. 2008. The quest for refined calibration of the Jurassic time-scale. *Proceedings of the Geologists' Association* **119**, 85–95.

PEARCE, J. A. 1982. Trace element characteristics of lavas from destructive plate boundaries. In: *Andesites. Orogenic Andesites and Related Rocks* (ed. R. S. Thorpe), pp. 525–49. Chichester: Wiley.

PELLENARD, P. & DECONINCK, J. F. 2006. Mineralogical variability of Callovo-Oxfordian clays from the Paris Basin and the Subalpine Basin. *Comptes Rendus Geoscience* **338**, 854–66.

PELLENARD, P., DECONINCK, J. F., HUFF, W., THIERRY, J., MARCHAND, D., FORTWENGLER, D. & TROUILLER, A. 2003. Characterization and correlation of Upper Jurassic (Oxfordian) bentonite deposits in the Paris Basin and the Subalpine Basin, France. *Sedimentology* **50**, 1035–60.

PRZYBYLSKI, P. A., OGG, J. G., WIERZBOWSKI, A., COE, A. L., HOUNSLOW, M. W., WRIGHT, J. K., ATROPS, F. & SETTLES, E. 2010. Magnetostratigraphic correlation of the Oxfordian-Kimmeridgian boundary. *Earth and Planetary Science Letters* **289**, 256–72.

RENNE, P. R., MUNDIL, R., BALCO, G., MIN, K. & MUDWIG, K. R. 2010. Joint determination of ^{40}K decay constants of ^{40}K decay constants and ^{40}Ar/^{40}K for the Fish Canyon sanidine standard, and improved accuracy for Ar-40/Ar-39 geochronology. *Geochimica et Cosmochimica Acta* **74**, 5349–67.

RENNE, P. R., MUNDIL, R., BALCO, G., MIN, K. & MUDWIG, K. R. 2011. Response to the comment by W. H. Schwarz *et al.* on "Joint determination of ^{40}K decay constants and ^{40}Ar*/^{40}K for the Fish Canyon sanidine standard, and improved accuracy for ^{40}Ar/^{39}Ar geochronology" by P.R. Renne *et al.* (2010). *Geochimica et Cosmochimica Acta* **75**, 5097–100.

SARTI, C. 1985. Biostratigraphie et faune à ammonites du Jurassique supérieur de la plate-forme atesine (Formation du Rosso Ammonitico Veronais). *Revue de Paléobiologie* **4**, 321–30.

SARTI, C. 1993. Il Kimmeridgiano delle Prealpi Veneto-Trentine: fauna e biostratigrafia. *Memorie del Museo Civico Storia Naturale di Verona* **5**, 9–144.

SELBY, D. 2007. Direct Rhenium-Osmium age of the Oxfordian-Kimmeridgian boundary, Staffin bay, Isle of Skye, U.K., and the Late Jurassic time scale. *Norwegian Journal of Geology* **47**, 291–9.

SPEARS, D. A., KANARIS-SOTIRIOU, R., RILEY, N. & KRAUSE, P. 1999. Namurian bentonites in the Pennine Basin, UK – origin and magmatic affinities. *Sedimentology* **46**, 385–401.

STEIGER, R. H. & JÄGER, E. 1977. Subcommission on geochronology: convention on the use of decay constants in geo-and cosmochronology. *Earth and Planetary Science Letters* **36**, 359–62.

THORPE, R. S., FRANCIS, P. W. & O'CALLAGHAN, L. 1984. Relative roles of source composition, fractional crystallization and crustal contamination in the petrogenesis of Andean volcanic rocks. *Philosophical Transactions of the Royal Society of London* **310**, 675–82.